PAPER

Online acoustic emission measurement of tensile strength and wear rate for AA8011-TiC- ZrB2 hybrid composite

To cite this article: Y Brucely *et al* 2022 *Surf. Topogr.: Metrol. Prop.* **10** 045009

Surface Topography: Metrology and Properties

PAPER

Online acoustic emission measurement of tensile strength and wear rate for AA8011-TiC- ZrB2 hybrid composite

RECEIVED
17 August 2022

REVISED
21 September 2022

ACCEPTED FOR PUBLICATION
17 October 2022

PUBLISHED
28 October 2022

Y Brucely[1,*], Y Christabel Shaji[2], A Bovas Herbert Bejaxhin[3] and Abeens M[4]

[1] Department of Mechanical Engineering, SRM TRP Engineering College, Irungalur, Tiruchirappali, Tamil Nadu, India
[2] Department of Chemistry, Holy Cross College (Autonomous), Nagercoil-629004, Tamil Nadu, India
[3] Department of Mechanical Engineering, Saveetha School of Engineering, SIMATS, Chennai, India
[4] Department of Mechanical Engineering, College of Engineering Guindy, Anna University, Chennai 600025, Tamil Nadu, India
[*] Author to whom any correspondence should be addressed.

E-mail: brucely2k6@gmail .com, christabelshaji@holycrossngl.edu.in and herbert.mech2007@gmail.com

Keywords: acoustic emission, tensile strength, hybrid metal matrix composite, SEM

Abstract

In current scenario the aircraft industry in need of a lightweight connecting material that persuade the technical and technological standards, but also need superior mechanical qualities. In this work the major objective is to enhance the strength behaviour of stir cast composites. Aluminum 8011 (Al 8011) titanium carbide (TiC) and zirconium boron (ZrB2) hybrid composites are stir cast in this work, and their microstructure, mechanical, and tribological properties are investigated. The matrix material was Al 8011, which was supplemented with stronger TiC to boost mechanical strength and softer ZrB2 to improve thermal and corrosion resistance without significantly changing electrical properties. According to the findings, the reinforced alloy's mechanical qualities outperform those of the unreinforced alloy. Acoustic energy generated during deformation of composite materials has been monitored and early fracture measurements has been achieved using the Acoustic emission (AE) approach in tensile test specimens. As a result of the experiment, Al8011 + 10% TiC + 2% ZrB2 composites outperform the Al8011 matrix alloy in terms of wear resistance, coefficient of friction, and surface smoothness, as well as other characteristics. The AFM representation of Al8011 + 10% TiC + 2% ZrB2 matrix reveals that the wear surface smoothness of the AMMC is significantly improved as compared to the Al8011 matrix alloys.

1. Introduction

Defects in the metal's surface pose substantial dangers to the mechanical system, reducing its overall strength significantly [1]. Metal matrix composites (MMCs) have acquired widespread recognition in a range of applications due to their better mechanical and tribological properties, which make them an attractive choice for many applications when compared to base alloys. Manufacturing vehicle and aircraft components using these manufactured materials has proven to be a lucrative business for them [2, 3]. Aluminum metal matrix composites (AMMCs) may be created by strengthening the soft ductile aluminium alloy with a second discontinuous phase, such as hard ceramic (oxides, carbides, borides, and nitrides) [4–9]. The mechanical behavior of materials, such as elastic modulus, yield and ultimate strengths, and elongation, must be well understood in order to apply them in manufacturing [9–15]. Due to their superior characteristics to aluminum alloys, AMMCs have long been explored for use in the automotive, aerospace, and architectural industries. The use of aluminum metal matrix composites is rapidly becoming an unavoidable and appealing material for advanced applications in a variety of industries such as aircraft, automobiles, textiles, marine, chemical, and general engineering. Particle-reinforced metal matrix composites (MMCs) have been the most widely used lightweight material during the past few years, with emphasis on enhancing the material's key technical characteristics (AMMCs). Despite this, low tensile strength, low hardness, and poor tribology are only a few of the issues that limit its ability to be used in a broad variety of applications. The Archimedean principle was used to determine the experimental density of composites, whereas the law

of mixing was used to get the theoretical density. Porosity, also known as the void fraction, is a measure of the void or empty spaces that are present in a material. Porosity is calculated as a proportion of the volume of voids relative to the total volume of the material [15–24]. The corrosion behavior of AA8011-ZrB2 composites was investigated using an *in situ* approach, and the presence of ZrB2 was verified using XRD and EDS. When AA8011 was exposed to NaCl solution, it was discovered that the addition of ZrB2 produced *in situ* inside AA8011 considerably improved corrosion resistance. Examinations of composites manufactured using the stir casting process using AA6063 and TiC (2, 4, 6, 8 and 10 percent) reveal that the inclusion of TiC particles decreased the composites' elongation and impact strength by 35 and 31 percent, respectively, while improving their hardness, density, and ultimate tensile strength by 20%, 7.8%, and 19.55%. [25–28]. The development of AMMCs may be accomplished by a variety of processes including stir casting, powder metallurgy, squeeze casting, and the molten salt stirring method. Nonetheless, in an effort to manufacture less expensive and more mass-produced materials, stir casting procedures have emerged as the most popular method used by researchers. Stir casting is preferred above all other processes due to its ease of use, low cost, and ability to produce homogenous particle dispersion inside the matrix. Stir casting is also less costly than other techniques [28–32]. The Taguchi approach was used to investigate the corrosion behavior of Silicon Carbide-reinforced Al6061 Aluminium metal matrix (AMMCs) composites. Al/SiC composites having 0%, 2%, and 4% SiC by weight were created using the stir casting process. The results showed that the presence of reinforcement particulates altered the microstructure of the matrix and served as a physical barrier to the onset and development of pitting corrosion. According to the EIS investigation, when TiC concentration rises, composites' polarisation resistance (Rp) increases [33, 34]. The characteristics of aluminium light alloys, especially TiB2 and AlB2, have been greatly enhanced by the use of boride-based ceramics like TiB2, AlB2, and ZrB2. This class of ceramic materials has distinguished itself from others and established itself as a prominent material used in industries to develop light alloys, particularly in the aerospace sector. This is due to their ability to improve alloy materials without eroding or degrading their intrinsic character. ZrB2 has a high melting point, great corrosion resistance, and a phenomenal strength mechanism because of the compound's strong covalent bonding [35–41]. The composites' characteristics will be improved by adding ZrB_2-Si3N4 reinforcement to aluminum alloy. Reinforcement of AMMCs with hard ceramic particles has been the subject of a great deal of research. According to previous studies, reinforcing particles improved mechanical characteristics while electrical properties boosted corrosion resistance and decreased wear rates [42–44]. Arya *et al* studied-on Al and Mg alloys using FSW process and reported FSW improved corrosion and mechanical strength of the surface of the material [45]. Qu, Shengguan, *et al* investigated on laser cladding process which improves wear property of the metal surface [46]. Lu, Ping *et al* reported Tribological behavior dominates in auto mobile and other machinery industries which leads to failure in mechanical components [47].

The stir casting process was used in this work to strengthen TiC and ZrB2 with Al8011alloy.Consequently, the primary emphasis of this research is on the characterization of hybrid composites by microstructural investigation, as well as mechanical parameters such as wear surface roughness, flexural, hardness, and acoustic energy generated during deformation has been monitored and early fracture identification has been achieved using the Acoustic emission (AE) approach in tensile test specimens was carried out. The following is the paper's main contribution: reinforcement of TiC and ZrB2 with Al8011alloy to increase mechanical and electrical characteristics, hybrid composites by microstructural analysis and tensile test specimen deformation has been tracked, and early fracture has been discovered.

2. Materials and methods

For the purpose of this study, the development of the binary composite consisting of AA8011-TiC-ZrB2 requires the use of a two-step stir casting technique that is carried out in accordance with [48]. The TiC particles and AA8011 base material with the chemical composition as shown in table 1 [49] required to synthesize composites with 0 percent, 5 percent, 1 wt percent, and 15% and 2 percent ZrB2 reinforcement are quantified. To improve wettability, the ceramic TiC and ZrB2 particle was heated to 450 °C to eliminate impurities, expel moisture, and degas the surface layer. The AA8011 alloy was subjected to temperatures that were 800 degrees Celsius higher than its melting point illustrate in figures 1(a) and (b), then the molten alloy was cooled to a semi-liquidus condition in the furnace before being charged with the prepared TiC - ZrB2 alloy. A melt pool of AA8011 was heated to 800 °C, and the slurry was agitated manually for 5 min before being heated again. The AA8011 melt pool was stirred with a mechanical stirrer at 300 rpm for approximately 10 min to ensure that the particulate was uniformly dispersed. In all, four samples from table 2 were subjected to the methods outlined above. To ensure that the molten composite had completely solidified, it was tilted into the sand mold for further solidification.

The molten composite was inverted into the sand mold for additional solidification to check that it had entirely formed. Figure 1(c) depicts the removal of the composites from the mold for subsequent processing.

Table 1. Chemicalcomposition of AA8011.

Si	Mn	Cu	Pb	Na	B	Zn	Fe	Mg	Ti	Al
0.46	.09	.14	0.01	.01	0.01	.22	0.61	0.47	0.01	Balance

Machining has been performed in accordance with the ASTM-E8M standard for hardness, wear, flexural and tensile test specimens' arrangement. Figure 1(d) depicts the ASTM-E8 standard-compliant processed specimen used in the aforementioned test.

2.1. Micro hardness measurement

The micro hardness of the created composites was measured using a Vickers micro hardness tester (Wolpert Wilson, 402 MVD) applied to the surface with a 50g force and a 5s dwell time. From the outer edge to the centre, the hardness was tested, and the average value was reported. The indenter makes contact with the surface of the specimen by impact. Because of this, the specimen material is capable of undergoing both elastic and inelastic deformations. It is possible to measure the deformation that occurs as a result of the kinetic energy of the indenter and that which remains. The value of the material's hardness may be calculated by taking the quotient of the test force and the size of the indentation for each of the four samples.

2.2. Wear test

Under dry sliding circumstances, the wear performance of several hybrid reinforced aluminum composites was assessed using the universal Tribometer S/N: RTEC 2441, USA. The pin-on-disc tribometer uses a ball made of E52100 alloy steel that is 25 inches in diameter. Thanks to meticulous grinding, the machined composite (specimen) with dimensions of 15 mm in diameter and 15 mm in length has smooth surfaces. The weight of the composite samples was determined prior to the test against a 350 mm diameter strong steel alloy. All other variables were maintained constant while the tribological experiment was carried out at the same sliding distance, time, and velocity of 3 mm s^{-1} while applying 20 N, 30 N, and 40 N. Both the friction force and coefficient of friction have been measured in this.

2.3. Flexural test

The flexural test was used to examine a material's response to being bent under a small amount of force. The specimen was made in compliance with the ASTM E290 standard's dimensions. The Flexural test on the ready composite was carried out using the universal Testing Machine. From its initial value of 0.5 KN all the way up to its breaking point, the load was gradually raised. The maximum load, flexural strength, and flexural modulus were all determined using the flexural test.

2.4. Tensile test

The tensile test was carried out with the aid of an Instron universal testing machine under a load of 30 KN while maintaining a crosshead speed of 2 m s^{-1}. In accordance with the specifications set out by ASTM, a composites specimen was created with cross-sectional dimensions of 5mm by 10mm and a gauge length of 30mm. This specimen was then put through the test.

2.5. Acoustic emission test

When a material experiences stress—also known as an internal change—as a direct result of an external force, a sound wave known as acoustic emission (AE) is created. This phenomenon is caused by the formation of elastic wave sources when a material is subjected to mechanical stress. Emissions originate from a slight displacement of a material's surface brought on by stress waves created when energy within a material or on its surface is rapidly released. When a material's surface or interior encounters a fast release of energy, stress waves are produced. In order to carry out the testing, an electro-mechanically operated UTM that was interfaced with an AE recorder was used.AE activity can be recorded with the use of AE sensors, which are then connected to a preamplifier and, after going through the appropriate filtering steps, posted as amplified signals. A sufficient frequency range is required of the filter in order to eliminate the undesired noise signal. Figure 2 Shows the experimental set up of acoustic emission.

The comparator receives filtered AE signals in addition to the threshold value.The AE platform acquisition system manufactured by Physical Acoustic Corporation was used in order to carry out continuous monitoring of the AE throughout the tensile testing (PAC). For this test, a piezoelectric-micro-80 type sensor with a resonance frequency between 175 kHz and 1 MHz was used. A threshold of 40 dB was used to exclude background noise. The AE resonant sensor was about in the middle of the tensile specimen, and the standard specimen was positioned between the UTM-grasping UNITEK-94100's grips [50].

3. Results and discussion

3.1. Study of Mechanical properties of AA8011

3.1.1. Hardness properties

The microhardness of composites made of AA8011/TiB-ZrB2 are shown in table 3. Due to the hybrid strengthening effect and volume proportion of ceramic boride and diboride in the composite alloy, composites with 20 percent weight of particles have

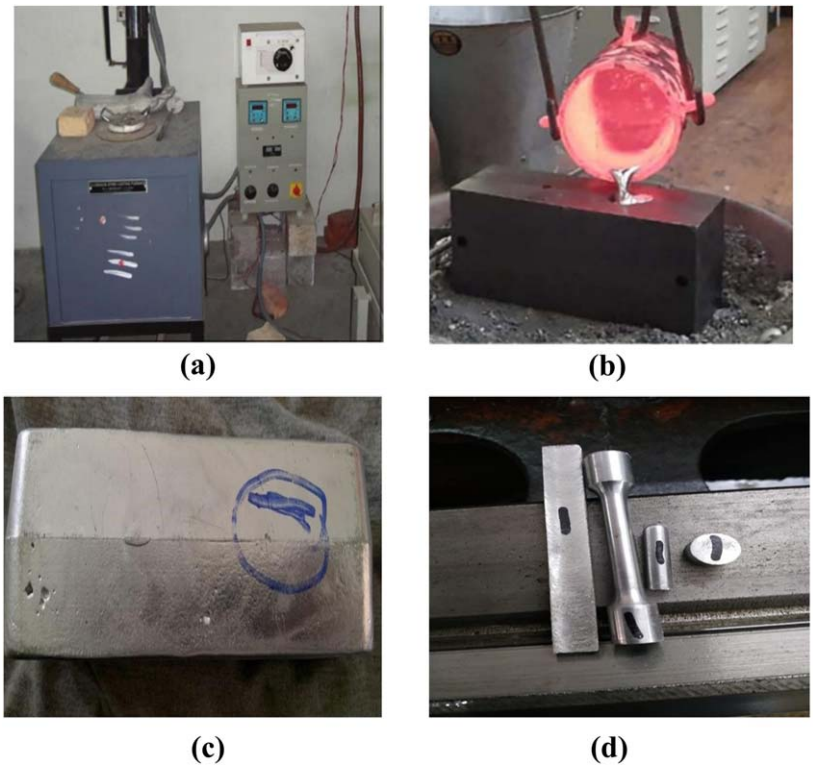

Figure 1. (a), (b) Arrangement of stir casting setup and the molten slag dispersion, (c), (d) Casted composite specimen and testing samples ASTM-E8.

the maximum hardness value. The hardness of the hybrid TiB-ZrB2 particles increases as the particulate volume % increases [49]. The TiB-ZrB2 hybrid particles operated as a heterogeneous nucleation site in the AA8011 matrix melt pool, leading to grain refinement and matrix hardening. TiB-ZrB2 hybrids present in the matrix are to be credited for the increased hardness, which improves the load-bearing capability of the metal matrix composite (AA8011/ TiB-ZrB2) as compared to the primary material (AA8011). Although the hybrid particulates and AA8011 have a strong intermetallic link due of their perfect wettability and homogeneity, this might also be responsible for the strengthening mechanism.

3.1.2. Flexural Strength

When shown in figure, the flexural strength of the composite formed with AA8081- TiC improves as the weight percent of TiC contained in MMCs increases. It has been discovered that increasing the quantity of TiC contained in an Al alloy enhances its flexural strength. The base alloy has a flexural strength that is 20% lower than that of the Al–15% TiC alloy, which shows the greatest flexural strength. The capacity to resist rupture is strengthened as a result of increases in the carbide content of TiC, as stated in [51].

The flexural strength is equal to the Al–15% TiC–2%ZrB2 flexural strength that was experienced inside the material just before it ruptured. When compared with the flexural strength of an AA8011–TiC– 2%ZrB2 composite, the flexural strength of an AA8011%–10% TiC–2% ZrB2 compositeis to be 10% lower figure 3. shows the wear testing setup. Experiments results of wear rate and Coefficient of friction are shown in table 4. Furthermore, the reinforcing materials have a substantial impact on the strength of the Al-TiC-Zr hybrid composites. This brittle and hard strength is the result of the matrix's dispersion hardening.

Table 2. Composites compositions.

Al 8011	TiC%	ZrB2%
Sample 1100	0	0
Sample 2 93	5	2
Sample 388	10	2
Sample 483	15	2

3.1.3. Wear and frictional analysis for Al 8011with various propositions of TiC and 2% ZrB2

According to the findings presented above, the mechanical properties hardness and flexural strength of the sample 3 composite are superior to those of the sample 1, sample 2 and the sample 4 composites, respectively. A wear and frictional study were carried out in order to find the best parameters for reducing the composite's wear and achieving the lowest possible coefficient of friction by making use of GRA. The experiments were carried out in accordance with the L9 OA as planned, and the results of the experiments were stated in table 2.

Figure 2. Experimental setup for acoustic emission.

Table 3. Micro hardness, Tensile strength and flexural strength values of composite samples.

Composites	Micro Hardness (BHN)	Flexural Strength (MPa)	Tensile Strength (MPa)
Sample 1 (Al 8011)	52.8	397	122
Sample 2 (Al 8011%–5%TiC-2%ZrB2)	53.6	405	180
Sample 3 (Al 8011%–10%TiC-2%ZrB2)	56.4	515	210
Sample 4 (Al 8011%–15%TiC-2%ZrB2)	55.8	523	230

3.1.4. Tensile strength of hybrid composites

The tensile test findings provided in figure 2 reveal that the ultimate tensile strength of the composite materials has grown since they were originally received when compared to the samples in their original form. It is obvious from the data that composites with a larger fraction of hybrid particle addition have greater strength. This improvement in strength is noticed in terms of the strengthening qualities outlined in [35]. It demonstrates how the ultimate tensile strength (UTS) of composites changes according on which sample 1–4 is used for reinforcement.

The composite material exhibits an increase in its ultimate tensile strength in comparison to the AA8011. As can be seen in figure 2, adding 10 percent by weight of TiC-ZrB2 results in a considerable improvement in the material's tensile strength. In general, the presence of hard ceramic particles (TiC-ZrB2) acting as a limitation to dislocation movement due to higher stress concentration near the matrix-reinforcement interface may be attributed to the mechanical property strengthening process [27, 35]. This is so that the dislocation movement is constrained by the tough ceramic particles. The tight packing of particles that takes place inside the ductile aluminium alloy AA8011 as a result of the alloy's better wettability may be the cause of the increased strength. This might be as a result of the improved wettability [34]. Due to the entire wettability between the matrix and the particle components, the unique interfacial properties of the matrix and the reinforcements dictate the characteristics of aluminium metal matrix composites. Furthermore, these characteristics are affected by the intermetallic bonding and adhesion that occurs between the matrix and the components of the particulates [35–39].

3.2. SEM micrograph

The microstructure of the coated surface, the distribution of the photocatalyst on the substrate surface, the uniformity, and the shape of the coating's particles are all revealed by scanning electron microscopy (SEM).

Figure 3. Wear testing set up—Pin on disc apparatus.

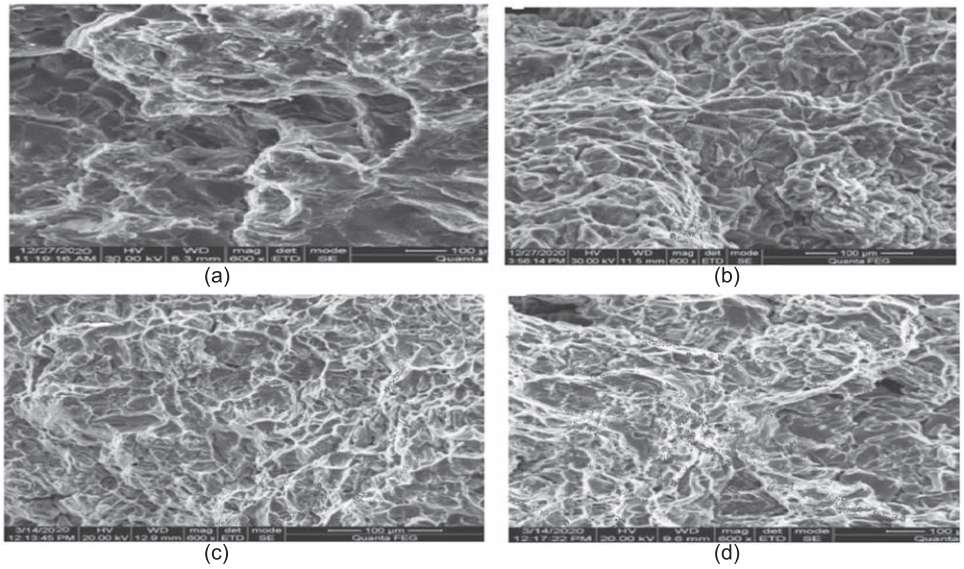

Figure 4. (a)–(d) SEM image for the samples 1–4 after tensile test.

Here it is used to identify the distribution of the reinforcement spread around the composite specimens. Figure 4(a) depicts that the pure alloy form of 8011 without any other solid substance. The dispersion of Ti and Zr particles in the form of closely packed white deposition cleanly visible inside the composite specimen as shown in figure 4(b) and (c). More amount of reinforcement have shown in figure 4(d) with more grain boundary by the blended effect of TiC and ZrB2.

3.3. Acoustic emission

3.3.1. Acoustic emission analysis

The acoustic setup and the AT post software were used to conduct an analysis of the acoustic emission (AE) data. Count, hits, voltage, and amplitude are the many AE metrics that may be collected from the test setup. These values are for samples 1, 2, 3, and 4. The transient AE signals may be distinguished from the background noise by their clearly defined beginning and ending positions for the bursts. Burst signals that originate from fracture or crack formation are the relevant signals for AE testing at varied weight percentages of composite material.

3.3.2. Acoustic emission waveform for various composites

Figure 5 depicts the corresponding AE waves generated for each of the various composites (a) -. (d). the portal's value is tuned such that it can filter out the noise signal produced by AE waves. An

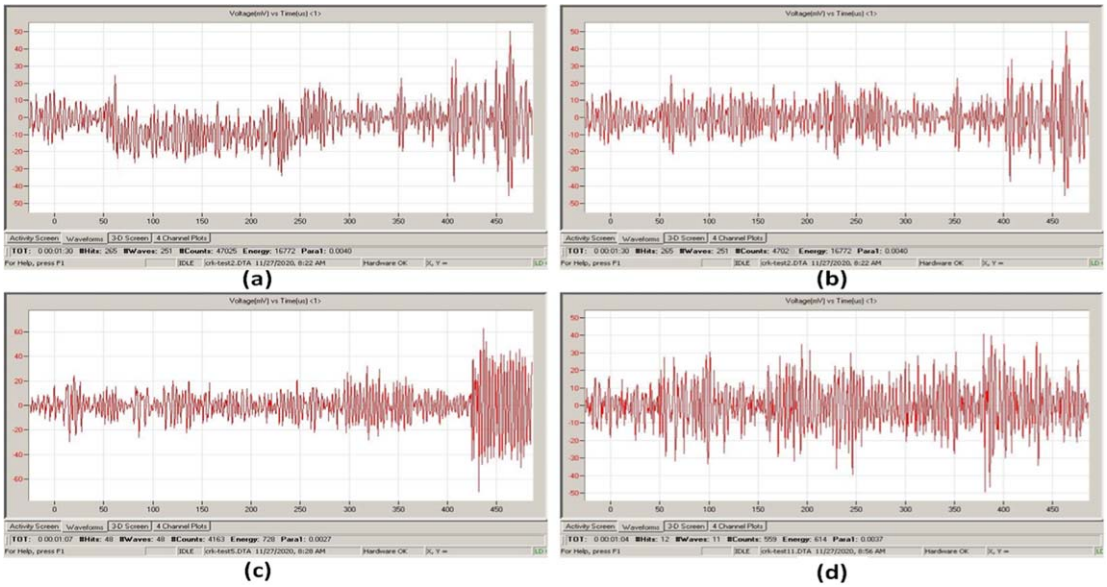

Figure 5. (a)–(d) Acoustic emission test results for the samples 1–4 voltagesvs time.

Table 4. Experiments results of wear rate and Coefficient of friction.

Sl.No	Loads (N)	Disc Velocity (m s)$^{-1}$	Sliding distance (m)	Wear rate (mm3 m)$^{-1}$	COF
1	10	1	500	0.00483	0.312
2	10	3	1000	0.00387	0.276
3	10	5	1500	0.00378	0.272
4	15	1	500	0.00247	0.325
5	15	3	1000	0.0046	0.288
6	15	5	1500	0.0067	0.363
7	20	1	500	0.00506	0.441
8	20	3	1000	0.00688	0.372
9	20	5	1500	0.00743	0.352

Al6061-containing composite's voltage versus time waveform is shown in figure 5(a). It was established that the threshold value was 4 mv. In 800 ms, the AE wave exceeded the threshold value more than 15 times. A pulse was produced when the AE wave went beyond the threshold. This pulse demonstrated that as the crack spread, energy was being released from within the material. This is the AE waveform of this was because there was a higher percentage of TiB2 in the composite, which indicates that there was a decrease in the propagation of cracks inside the material as a result of the rise in the percentage of TiC. The AE wave shape is shown in figures 5(c) and (d), respectively, for samples 3 and 4. The waveforms show that the fracture grows gradually and that energy was being produced in the phases prior to the break being discovered. These details may be gleaned from the waveforms. Additionally, it was shown that introducing more TiB2 and Gr particles slowed the pace at which internal fractures propagated. The fundamental reason for this is the effect that TiC and ZrB2 reinforcement has. It helps to prevent the formation of fractures inside the material. The results of this experiment agreed with those of a prior investigation on the same base metal [52, 53].

3.3.3. Acoustic emission distribution for various composites

Every cycle, an AE occurrence is referred to as a hit. A hit happens when a signal reaches a level greater than the threshold, causing a system channel to start collecting data. Figure 5 displays the composite's effect versus time waveform with varied proportions. This waveform is seen in the preceding graphic (a)–(d). If the composite has high strength and a long life, this figure shows that fractures begin slowly and propagate progressively over time. The conclusion may be drawn from figure 5(c), which shows that the fractures appear later in the testing process compared to the other composites. The fact that sample 3 has an excellent tensile strength is supported by this piece of data. Figures 5(a), (b), and (d) show that the hit begins at 8 s for sample 3, 16 s, and 19 s, respectively. Additionally, it has been noted that adding additional TiC mixed with ZrB2 particles to the composite delays the start of impact events.

3.3.4. Hit amplitude versus time plot in 3D for composites

Figures 6(a)–(d) depicts the results of the hit-amplitude distribution as a function of time of manifestation. It shows the Acoustic Emission distribution in three dimensions for samples 1 through 4. The inclusion of TiC and ZrB2 results in an increase in amplitude, which is confirmed by all of the 3D surfaces. The AE distribution is shown in figures 6(a)

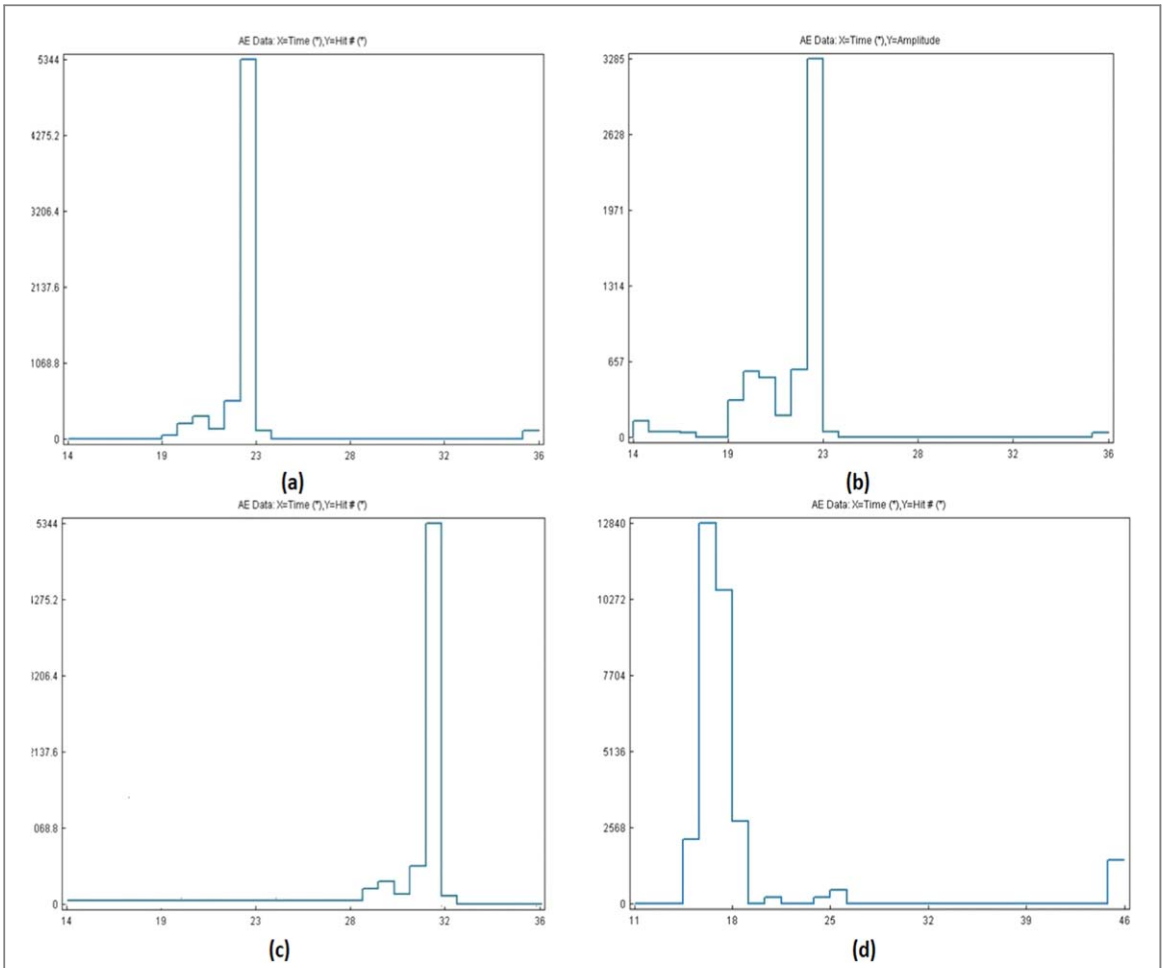

Figure 6. (a)–(d) Acoustic emission distribution for samples 1–4 (hits versus time).

and (b), which may be found by referring to that image. All of the numbers make it clear that there was a small number of AE events with a low amplitude that were recorded prior to the first crack opening as well as the final cracking. Even though the composite produced a large number of high-amplitude events, these occurrences may be categorized as micro-scale events with little to no energy.

Figure 7 demonstrates how comparing the hit amplitude distribution across the samples in respect to the time of occurrence revealed that the tests were quite comparable to one another. During the course of the testing, it is clear that there was an extremely high volume of impacts of moderate amplitude. The AE amplitudes have reached a maximum value as the amount of TiC and ZrB2 particles in the composite representation. After reaching this maximum value, the amplitudes began a fast decline that lasted until the composite failed completely. This is because of their tough character and the strong bonds they have.

4. Conclusion

In the present investigation, tensile specimen characterization, acoustic analysis, and wear friction analysis of Al 8011 Mg and TiC–ZrB2 composites were conducted. On the basis of the analysis, the following conclusions were carried out.

1. Using the stir casting process, effective preparations of Al 8011 and TiC–ZrB2 composites were achieved.
2. The hardness, flexural and tensile strength of composites improved noticeably due to TiC with ZrB2 concentration increased.
3. The hardness of the Al 8011%–10%TiC-2%ZrB2 sample seems to be much higher than that of the other composites.
4. Due to the addition of TiC to ZrB2 significantly lowered the composites' wear rate.
5. According to the AE investigation, the incorporation of TiC-ZrB2 made the material more resistant to internal fractures.
6. The mechanical and tribological characteristics of hybrid composites were shown to be superior to those of single reinforced composites. Al8011and TiC-ZrB2 hybrid composite exhibited significantly improved hardness, ultimate tensile strength, and wear resistance as compared to unreinforced Al8011

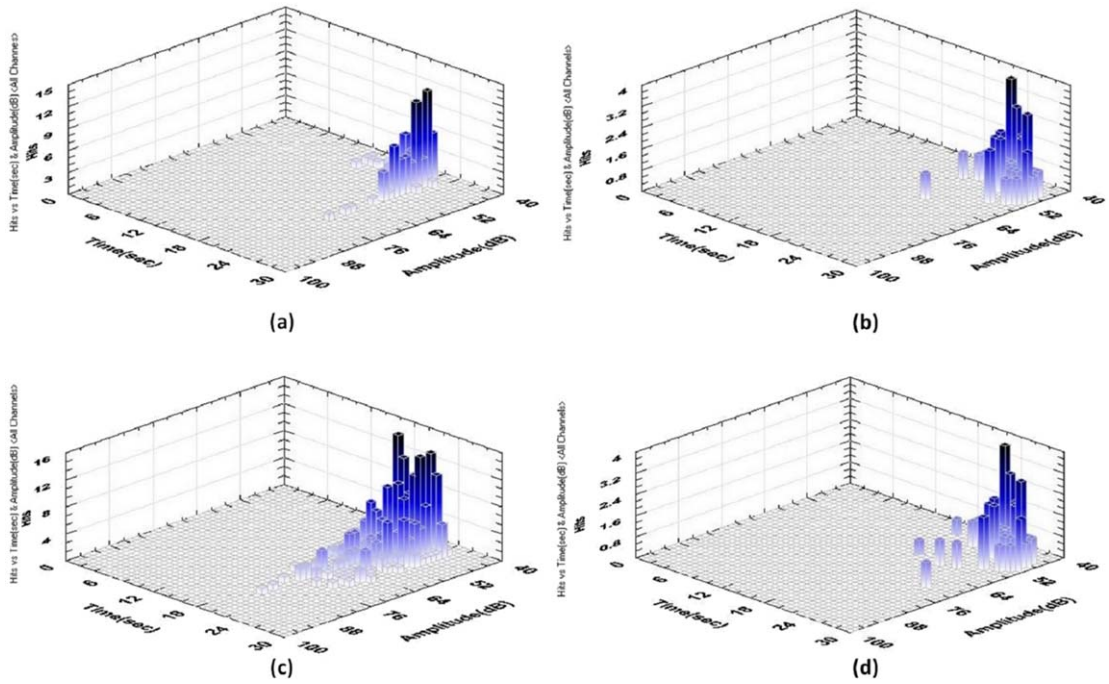

Figure 7. (a)–(d) 3-Dimensional distribution for composites samples 1–4.

alloy. As a result, the hybrid composite has the potential to be used in the aerospace sector due to the fact that it has superior mechanical and tribological qualities.

Data availability statement

All data that support the findings of this study are included within the article (and any supplementary files).

ORCID iDs

Y Brucely https://orcid.org/0000-0002-3965-1690
Abeens M https://orcid.org/0000-0001-6368-5498

References

[1] Wei-Yu C, Yu-Reng T, Jin-Yi L, Ching-Jung H, Yu-Cheng L and Cheng-Yang L 2022 Real-time instance segmentation of metal screw defects based on deep learning approach *Measurement Science Review* **22** 107–11
[2] Anand Partheeban C-M, Rajendran M, Vettivel S C, Suresh S and Moorthi N-S-V 2015 Mechanical behavior and failure analysis using on line acoustic emission on nano-graphite reinforced Al7075–10TiB2 hybrid composite using powder metallurgy *Materials Science & Engineering A* **632** 1–13
[3] Arif S, Alam M T, Ansari A-H, Siddiqui M-A and Mohsin M 2017 Study of mechanical and tribological behaviour of Al/SiC/ZrO_2 hybrid composites fabricated through powder metallurgy technique *Mater. Res. Express* **4** 076511
[4] Babalola P O, Inegbenebor A O, Bolu C A and Inegbenebor 2015 The development of molecular based materials for electrical and electronic application *J Miner. Met Miner Soc (TMS)* **67** 830–4
[5] Abeens M, Muruganatham R and Arulvel S 2019 *Indian. J. Eng. Mater. S.* **26** 20
[6] Abeens M, Meikandan M, Sheriff J and Murunganadhan R 2020 *Int. J. Ambient Energy* **41** 540
[7] Thirumavalavan K *et al* 2019 Study on the influence of process parameters of severe surface mechanical treatment process on the surface properties of AA7075 T651 using TOPSIS and Taguchi analysis *Mater. Res. Express* **6** 1165i1
[8] Abeens M, Muruganandhan R and Thirumavalavan K 2020 Effect of Low energy laser shock peening on plastic deformation, wettability and corrosion resistance of aluminum alloy 7075 T651 *Optik* **219** 165045
[9] Abeens M *et al* 2020 Experimental analysis of convective heat transfer on tubes using twisted tape inserts, louvered strip inserts and surface treated tube *Int. J. Ambient Energy* **41** 540–6
[10] Podgornik B, Žužek B, Sedlaček M, Kevorkijan V and Hostej B 2016 Analysis of factors influencing measurement accuracy of Al alloy tensile test results *Measurement Science Review* **16** 1–7
[11] Abeens M *et al* 2021 An investigation on the effect of stacking fault energies on surface mechanical treatment process of AA6061 alloy and ETP-copper *Surface Topography: Metrology and Properties* **9** 035010
[12] Sastry C C *et al* 2020 Microstructural analysis, radiography, tool wear characterization, induced residual stress and corrosion behavior of conventional and cryogenic trepanning of DSS 2507 *J. Mech. Sci. Technol.* **34** 2535–47
[13] Premnath M, Muruganandhan R and Abeens M 2022 A study on the effect of various process parameters on low pulsed energy of laser shock peening without ablative layer on the mechanical behavior of AA 7075 T651. *Surface Topography: Metrology and Properties* **10** 015044
[14] Abeens M *et al* 2019 Surface modification of AA7075 T651 by laser shock peening to improve the wear characteristics *Mater. Res. Express* **6** 066519
[15] Kumar R and Das A K 2022 Tribological behavior of TiB2 ceramic based composite coating deposited on stainless steel AISI 304 by gas tungsten arc (GTA) cladding process *Surface Topography: Metrology and Properties* Surf. Topography **10** 10
[16] Dwivedi P, Siddiquee A N and Maheshwari S 2021 Issues and requirements for aluminum alloys used in aircraft components: state of the art *Russian Journal of Non-Ferrous Metals* **62** 212–25
[17] Karthik B-M, Gowrishankar M-C, Sharma S, Hiremath P and Shettar M 2020 Coated and uncoated reinforcements metal

matrix composites characteristics and applications—a critical review *Cogent Engineering* **7** 1–18
[18] Shendur G S, Abeens M, Muruganadhan R, Arivanandhan M, Premnath M and Rajasekaran E 2020 *Mater. Today. Conf. Proc.* **22** 879
[19] Dai D *et al* 2022 Analysis of surface quality and optimization of process parameters in laser-assisted cutting of SiC ceramics *Surface Topography: Metrology and Properties* (https://doi.org/10.1088/2051-672X/ac849b)
[20] Wood R and Costa H L 2022 STMP at 10: shaping surface metrology, measurement and phenomena for a decade *Surface Topography: Metrology and Properties* **10.2** 020201
[21] Brunatto S F 2022 Surface state change influence's theoretical approach of pressed iron on hollow cathode discharge characteristics: first results of plasma heating reproducibility for sintering purposes *Surface Topography: Metrology and Properties* (https://doi.org/10.1088/2051-672X/ac84f4)
[22] Ovsik M *et al* 2022 The influence of tool's surface topography on mechanical properties of injection moulded product *Surface Topography: Metrology and Properties* (https://doi.org/10.1088/2051-672X/ac843c)
[23] Rosenkranz A and Marian M 2022 Combining surface textures and MXene coatings–towards enhanced wear-resistance and durability *Surface Topography: Metrology and Properties* (https://doi.org/10.1088/2051-672X/ac7f4a)
[24] Alam M T 2020 Physical, corrosion and microstructural analysis of A356/SiC nanocomposites fabricated through stir casting process *Mat. Sc. Forum* **1034** 73–86
[25] Kenneth K, Alaneme A V F and Nthabiseng Beauty Maledi 2018 Development of aluminum-based composites reinforced with steel and graphite particles: structural, mechanical and wear characterization *J Mater Res Tech.* 1856758
[26] Shankar B-L, Nagaraj P –M and Anil K-C 2017 Optimization of wear behavior of AA8011-Gr composite using taguchi technique *Mater. Today Proc.* **4** 10739–45
[27] Selvan B –M and Anandakrishnan V 2019 Investigations on corrosion behaviour of AA 8011- ZrB2 *in situ* metal matrix composites advances in manufacturing technology. ed s hiremath *Advances in Manufacturing Technology*
[28] Kumar K-R, Kiran K and Sreebalaji V-S 2017 Microstructural characteristics and mechanical behaviour of aluminium matrix composites reinforced with titanium carbide *J. Alloys . Compd* **723** 795–801
[29] Moses J-J, Dinaharan I and Sekhar S-J 2016 Prediction of influence of process parameters on tensile strength of AA6061/TiC aluminum matrix composites produced using stir casting *Trans. Nonferrous Met. Soc. China* **26** 1498–511
[30] Pan S, Sokoluk M, Cao C, Guan Z and Li X 2019 Facile fabrication and enhanced properties of Cu-40 wt% Zn/WC nanocomposite. WC nanocomposite *J. Alloys Compd.* **784** 237–43
[31] Kumar S, Subramanian R, Shalini S, Anburaj J and Angelo P-C 2016 Synthesis, microstructure, and mechanical properties of Al-Si-Mg hybrid (zircon+alumina) composites *Indian Journal of Engineering & Materials Sciences* **23** 20–6
[32] Alaneme K-K and Bodunrin M-O 2013 *Mechanical behavior of alumina reinforced aa 6063 metal matrix composites developed by two steps—stir casting processActa Technical Conveniences, Bulletin of Engineering.* (https://acta.fih.upt.ro/issues.html)
[33] Sarapure S, Shivakumar B-P and Hanamantraygouda M-B 2020 Investigation of corrosion behavior of SiC-reinforced Al 6061/SiC metal matrix composites using taguchi technique *Journal of Bio- and Tribo-Corrosion* **6** 2020
[34] Ananda Murthy H-C and Singh S-K 2015 Influence of TiC particulate reinforcement on the corrosion behavior of Al 6061 metal matrix composites *Advanced Materials Letters* **6** 633–40
[35] Jeyaprakasam S, Venkatachalam R and Velmurugan C 2019 Experimental Investigations on the influence of TiC/graphite reinforcement in wear behavior of Al6061 hybrid composites *Surf. Rev. Lett.* **26** 1850173
[36] Fayomi J, Popoola A-P-I, Popoola O-M and Fayomi O-S-I 2019 Influence of zirconium diboride (ZrB2) on the physio-mechanical properties of high-grade AA8011 metal matrix composites *J. Phys. Conf. Ser.* **1378** 032044
[37] Vasanth K-R, Keshavamurthy R and Chandra P-S 2016 . *Microstructure and mechanical behaviour of Al6061-ZrB2 in situ metal matrix composites. IOP Conf. Ser. Mater. Sci. Eng. 149 . 012062. 587*
[38] Selvan B-M-M, Veeramani A and Muthukannan D 2018 Investigation of tribological behaviour of AA8011-ZrB2 *in situ cast-metal-matrix composites.MTAEC9* **52** 451
[39] Neuman E-W 2014 Elevated Temperature Mechanical Properties of Zirconium Diboride Based Ceramics. *Missurouri S and T Library and learning tools* Missouri University of Science and Technology (https://scholarsmine.mst.edu/doctoral_dissertations/2164?utm_source=scholarsmine.mst.edu%2Fdoctoral_dissertations%2F2164&utm_medium=PDF&utm_campaign=PDFCoverPages)
[40] Gautam G and Mohan A 2015 Effect of ZrB2 particles on the micro-structure and mechanical properties of hybrid (ZrB2 þ Al3Zr)/AA5052 *in situ* composites *J. Alloys Compd.* **649** 174–83
[41] Ravi B 2017 Fabrication and mechanical properties of Al7075-SiC-TiC hybrid metal matrix composites *Int. J. Eng. Sci.In.* **6** 10
[42] Ul Haq M I and Anand A 2018 Dry sliding friction and wear behavior of AA7075-Si3N4 composite *Springer Science +Business Media B.V., part of Springer Nature* 2018
[43] Kandan R-J, Kumar D, Sudharssanam M, Venkadesan and Badrinath R 2017 Investigation of mechanical properties on newly formulated hybrid composite aluminium 8011 reinforced with B4C and Al_2O_3 by stir casting method.2017 *Int. J. Sci. Res.dev.* **5** issue 01
[44] Popoola A-P-I, Pityana S-L and Popoola O-M 2011 Microstructure and corrosion properties of Al (Ni/TiB2) intermetallic matrix composite coatings *J. S. Afr. Inst. Min. Metall. [online].* **111** 345–53
[45] Kumar A , P *et al* 2022 Microstructure, mechanical and corrosion properties of differently cooled friction stir welded joints of Al and Mg alloys *Surface Topography: Metrology and Properties* (https://doi.org/10.1088/2051-672X/ac8365)
[46] Qu S *et al* 2022 Improvement of impact wear properties of seat insert by laser cladding cobalt-based alloy *Surface Topography: Metrology and Properties* **10** 035015
[47] Lu P and Robert J K W 2020 Tribological performance of surface texturing in mechanical applications—a review *Surface Topography: Metrology and Properties* **8.4** 043001
[48] Babaremu K-O, Joseph O-O, Akinlabi E-T, Jen T-C and Oladijo O-P 2020 Morphological investigation and mechanical behaviour of agrowaste reinforced aluminium alloy 8011 for service life improvement *Heliyon.* **6** e05506
[49] Fayomi J, Popoola A-P-I, Popoola O-M and Fayomi O-S-I 2019 Tribological and microstructural investigation of hybrid AA8011/ZrB2 -Si3N4 nanomaterials for service life improvement *Results Physics* **14** 102469
[50] Sam M, Jojith R and Radhika N 2021 Progression in manufacturing of functionally graded materials and impact of thermal treatment—A critical review *Journal of Manufacturing Processes* A **68** 1339–77
[51] Baskaran S, Anandakrishnan V and Duraiselvam M 2014 Investigations on dry sliding wear behavior of *in situ* casted AA7075–TiC metal matrix composites by using Taguchi technique *Materials & Design* **60** 184–92
[52] Poria S, Sutradhar G and Sahoo P 2017 Design of experiments analysis of friction behavior of Al-TiB_2 composite **4** Part A, 2017 2956–64
[53] Partheeban A, Madhumitha Rajendran C-M, Vettivel, S-C and Suresh S 2015 Mechanical behavior and failure analysis using online acoustic emission on nano-graphite reinforced Al6061–10TiB_2 hybrid composite using powder metallurgy *Materials Science & Engineering A* **632** 1–13